Atmospheric Environment 101 (2015) 1–9

Contents lists available at ScienceDirect

Atmospheric Environment

journal homepage: www.elsevier.com/locate/atmosenv

Theoretical model on the formation possibility of secondary organic aerosol from ·OH initialed oxidation reaction of styrene in the presence of O_2/NO

Honghong Wang [a, b, 1], Yuemeng Ji [a, 1], Yanpeng Gao [a, b], Guiying Li [a], Taicheng An [a, *]

[a] State Key Laboratory of Organic Geochemistry and Guangdong Key Laboratory of Environmental Resources Utilization and Protection, Guangzhou Institute of Geochemistry, Chinese Academy of Sciences, Guangzhou 510640, China
[b] University of Chinese Academy of Sciences, Beijing 100049, China

HIGHLIGHTS

- Mechanism and kinetics of ·OH initiated oxidation of styrene were investigated.
- DFT was applied to predict the possibility of SOA formation.
- The dependence of $\tau_{1/2}$s on temperature and the altitude were attempted.

GRAPHICAL ABSTRACT

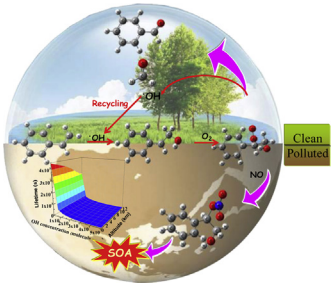

ARTICLE INFO

Article history:
Received 3 September 2014
Received in revised form
14 October 2014
Accepted 24 October 2014
Available online 24 October 2014

Keywords:
Styrene
·OH initiated oxidation
SOA formation
Theoretical study
Mechanisms
Kinetics

ABSTRACT

Understanding ·OH oxidation reaction is vital in understanding atmospheric pollution dynamics, and developing possible strategies for countering pollutant problems. This study used a theory-based approach to model the formation mechanisms of secondary organic aerosol (SOA) from styrene-·OH oxidation reactions in the presence of O_2/NO. As a comparative measure, the mechanisms in the absence of NO (representing a pollution-free environment) were also investigated. The results showed that styrene can be initially attacked by ·OH in two ways: OH-addition and H-abstraction. The OH-aliphatic-addition pathway occurs easily; the H-abstraction pathway may be ignored given atmospheric conditions. It was found that $IM_{add}\beta$ ($C_6H_5CHCH_2OH$) was the main intermediate, and could be transformed to a peroxyl radical in the presence of O_2. In the NO-free atmosphere, the peroxyl radical was decomposed to recycling-·OH and aldehydes. In the NO-polluted atmosphere, it could be degraded to organic nitrate ($RO\text{-}NO_2$) which plays an important role in the production of SOA. Besides, the percent of organic nitrate in the particulate phase was calculated within the range of 2.4%–6.3% in Guangzhou city, and organic nitrates may constitute an important fraction of the total organic aerosol. The kinetic data calculated using canonical variational transition state theory with the small-curvature tunneling correction showed that, in the NO-polluted/unpolluted atmospheres, the styrene-·OH oxidation reaction easily occurred across an altitude range of 0–12 km. Especially, peroxyl radical lifetime was 10^{-3} s in the high NO-

* Corresponding author.
E-mail address: antc99@gig.ac.cn (T. An).
[1] Both authors contributed equally to this work and were considered co-first authors.

http://dx.doi.org/10.1016/j.atmosenv.2014.10.042
1352-2310/© 2014 Elsevier Ltd. All rights reserved.

polluted atmosphere, indicating that the styrene-•OH oxidation reaction could significantly contribute to SOA formation in the NO-polluted atmosphere. The current results informed possible approaches for forming SOA from volatile organic compound (VOC) oxidation reactions, and could help evaluate regional air quality, especially in high NO-polluted atmospheres.

© 2014 Elsevier Ltd. All rights reserved.

1. Introduction

Styrene is a well known volatile organic compound (VOC) with abundant anthropogenic and natural emission sources. It can be released into atmosphere from building materials (Uhde and Salthammer, 2007), consumer products, tobacco smoke (ATSDR, 2007), and industrial applications (ATSDR, 2007; Guo et al., 2012). It can also be found widely in nature, such as in plants (Baxter and Warshawsky, 2012) and microorganisms (ATSDR, 2007). As such, styrene can be frequently detected in both outdoor and indoor environments, especially in the industrialized areas of developing countries (Tan et al., 2012a; Uhde and Salthammer, 2007). As early as 1990, styrene was identified as a hazardous air pollutant by the Clean Air Act (Tuazon et al., 1993); it is also listed as a pollutant by the U.S. Environmental Protection Agency (EPA) due to its potential mutagenic and carcinogenic properties (EPA, 2013).

Because of its unsaturated characteristics, styrene is highly reactive in the atmosphere, and can be attacked readily by reactive oxygen species (ROSs), such as hydroxyl radical (•OH), O_3, and nitrate radical ($^{\bullet}NO_3$). This results in secondary pollution. For example, a styrene-ozone oxidation reaction could form secondary organic aerosol (SOA) (Na et al., 2006). However, among these ROSs, reacted with •OH has been estimated to be the most important loss process for styrene in the daytime at ambient atmospheric conditions (Tuazon et al., 1993). As such, the contribution of styrene-OH oxidation reaction to the formation of atmospheric SOA could be more significant than other styrene-ROSs reactions.

The styrene-OH oxidation reaction has been investigated in previous experiments (Atkinson and Aschmann, 1988; Bignozzi et al., 1981; Sloane and Brudzynski, 1979), but these studies only focused on identifying the atom of styrene which is most likely to be attacked by •OH and thus predicting the easiest initial reaction in the atmosphere. For example, Sloane and Brudzynski (1979) reported that •OH would most likely attack both the ring and side chain of styrene, but Bignozzi et al. (1981) noted that only the styrene side chain was more susceptible to OH oxidation. In these studies, the rate constant of the initial reaction was measured to be at the magnitude of 10^{-11} cm^3 $molecule^{-1}$ s^{-1}, suggesting that the initial reaction of •OH with styrene could occur quite easily, and the effect of this oxidation reaction on the atmosphere should not be ignored (Atkinson and Aschmann, 1988; Bignozzi et al., 1981). However, up to date, no experimental and theoretical investigations were conducted to probe the SOA formation possibility from these atmospheric reactions.

On the other hand, nitrogen oxides (NO_x) are a ubiquitous trace gas, widely found in the polluted atmosphere. Organic nitrate, observed in ambient atmospheric aerosol, are produced by the oxidation of various VOCs in the presence of NO_x (Renbaum and Smith, 2009). Experimental evidence has shown that NO_x concentrations may significantly influence SOA formation. For example, isoprene photooxidation may contribute to 0.9–3.0% and ~3% SOA yields at high and low NO_x levels, respectively (Kroll et al., 2005, 2006). If the NO_x concentration is less than 4.61×10^{15} molecule cm^{-3} (100 pptv), NO is estimated to account for one third of NO_x. Under other conditions, NO dominates NO_x species (Clapp and Jenkin, 2001). Given this, in this work, the formation possibilities of SOA from styrene-OH oxidation reaction was comprehensively compared in the absence and presence of NO, using a theory-based approach. Several other factors that influence SOA formation as well, including temperature, O_2 concentration, and the altitude was also considered. Using canonical variational transition state theory (CVT) with small curvature tunneling (SCT) correction, the kinetics were also calculated within the atmospheric temperature range of 216–298 K. Besides, the atmospheric gas-particle partitioning of final product organic nitrate was predicted by the K_{oa} model, which can help us to better understand the SOA formation in this oxidation system. Calculated results were validated with the available experimental data to assess proposed model reliability. The current obtained results might inform the establishment of an atmospheric model of SOA formation and estimate the contribution of styrene-•OH oxidation reactions to the atmospheric chemistry pollution.

2. Methods

All quantum chemical calculations were performed with Gaussian 03 software package (Frisch et al., 2003). The geometries of all stationary points, including reactants, intermediates (*IM*s), transition states (*TS*s), and products were optimized at the B3LYP/6-311G(d, p) level, because our group (An et al., 2014; Gao et al., 2014) and other groups (Sun et al., 2012) have achieved reliable results using the B3LYP hybrid functional method to study molecule-radical oxidation systems. At the same level of theory, the harmonic vibrational frequencies were calculated to determine the nature of stationary points, the zero-point energy (ZPE), and the thermal contribution (TC). The intrinsic reaction coordinate (IRC) (Fukui, 1981) analysis was carried out to confirm that the transition state indeed connected with the corresponding minimum stationary points associated with reactants and products. The potential energy surface (PES) was refined at the B3LYP/6-311+G(3df, 3pd) level, including ZPE correction based on the geometries obtained by the B3LYP/6-311G(d, p) level, denoted as B3LYP//B3LYP. The comparison shows that the B3LYP//B3LYP level of theory get a balance between accuracy and the computational cost. And full discussion is provided in Supporting information. The force constant matrices of stationary points and the selected nonstationary points near the *TS* along the Minimum-Energy-Path (MEP) were also calculated to obtain kinetics results. Kinetics were obtained using canonical variational transition state theory (CVT) (Gonzalezlafont et al., 1991) with the small curvature tunneling (SCT) correction (Fernandez-Ramos et al., 2007), denoted as CVT/SCT, which has been successfully used to calculate bimolecular reactions (Ji et al., 2012, 2013). Using the Polyrate program (Corchado et al., 2002), the initial information on the PES was used to evaluate the rate constants within the atmospheric temperature range of 216–298 K. The half-life ($\tau_{1/2}$) of the titled reaction was calculated using the formula $\tau = \ln 2/(k[A])$, where k denotes the rate constant, and [A] is the concentration of •OH, O_2 or NO. The influence of the altitude on rate constants was also considered from the surface of the earth to the stratosphere. In the troposphere, the

temperature drops about 6.49 K for every 1 km increase in altitude (Ji et al., 2013). Into the stratosphere (from 11 km height above the earth surface), the constant temperature is 216.69 K. According to this temperature–altitude relationship, the rate constant at different altitude was deduced from the temperature-dependence rate constant, thus the half-life at different altitude was also obtained.

3. Results and discussion

3.1. Initial reaction of styrene with ·OH

3.1.1. Reaction mechanisms

The stationary point geometries involved in the initial reaction of styrene with ·OH are presented in Figs. S1–S3. For meaningful comparison, some available experimental data (Molina et al., 1999) are also listed in Fig. S1. To further confirm the calculated geometry corresponding to a saddle point with only one imaginary frequency or a local minimum without imaginary frequency, the harmonic vibrational frequencies of the main stationary points and experimental values are listed in Table S1. These figures and table show that the geometry parameters and frequencies calculated at the B3LYP/6-311G (d, p) levels align well with the available experimental data (Molina et al., 1999), suggesting that the calculated structural parameters at the B3LYP level are reliable. As shown in Fig. S1, C_1 symmetry can be found, but the side chain and benzene ring of styrene are almost in the same plane ($\tau(C_1C_6C_\alpha C_\beta) = 179.98°$). Therefore, eight OH-addition (R_{add}) and seven H-abstraction (R_{abs}) pathways were identified and are depicted in Scheme S1. The potential energy surfaces of all R_{add} and

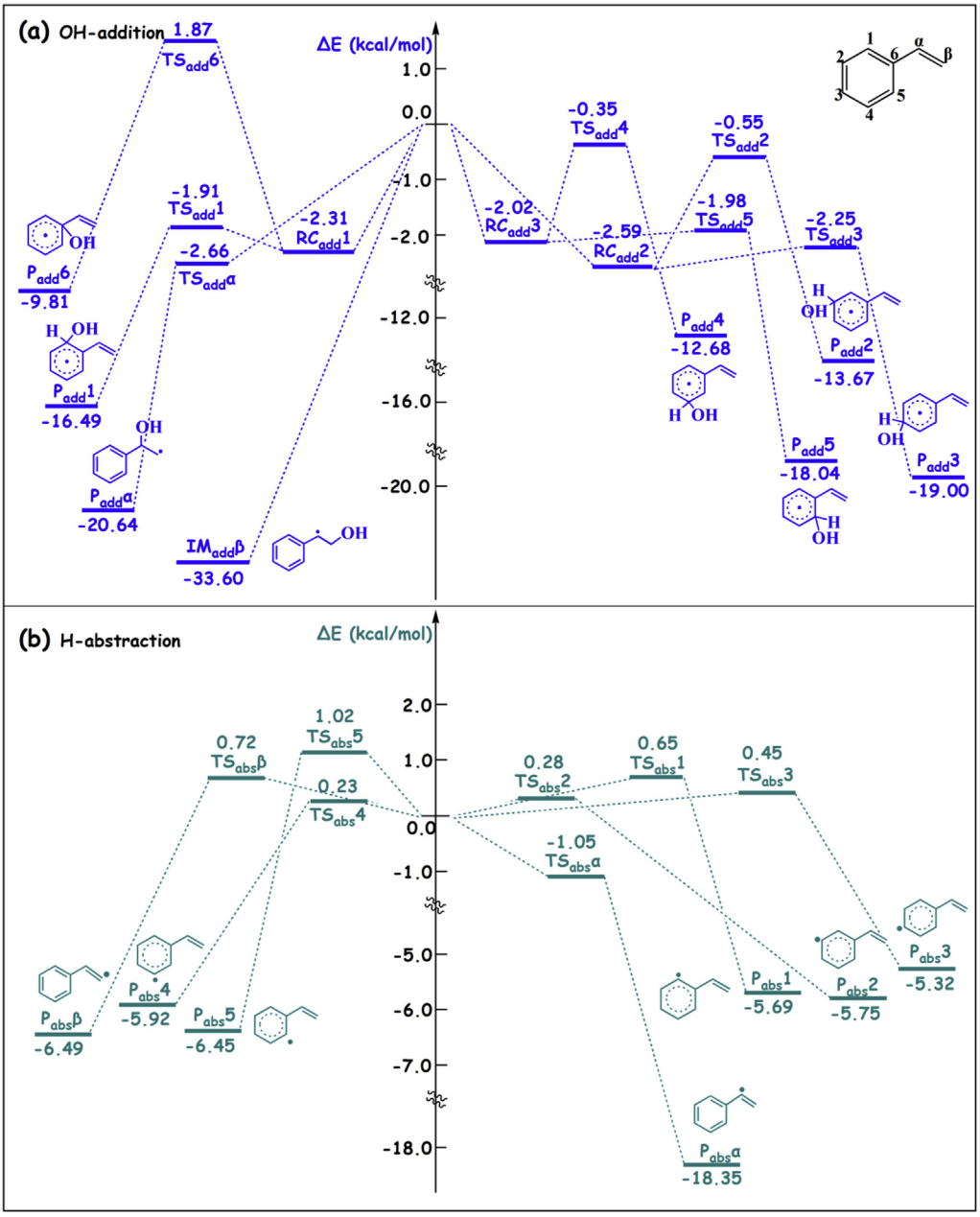

Fig. 1. Potential energy surface of (a) OH-addition pathways and (b) H-abstraction pathways.

R_{abs} pathways were constructed at the B3LYP/6-311+G(3df, 3pd)//B3LYP/6-311G (d, p) level (Fig. 1).

For R_{add} pathways, six carbon sites in the benzene ring and another two carbon sites in the aliphatic chain could be attacked by ·OH, denoted in this study as OH-benzene-addition (R_{add}1-6) and OH-aliphatic-addition ($R_{add}\alpha$-β) pathways (Scheme S1). From Fig. 1a and Table S2, it is clear that the $R_{add}\beta$ pathway could readily occur in the atmosphere because it is a barrierless process (Fig. S4) with exothermic energy of −33.60 kcal/mol. However, although other OH-addition pathways were all barrier processes, these pathways could not be ignored in the atmosphere, because the energy barriers (ΔE) of them were almost negative. This similar behavior can also be found from other reaction systems of ·OH addition to compounds contained phenyl group (Seta et al., 2006). Except for the $R_{add}6$ pathway, the ΔEs of the R_{add}1−5 and $R_{add}\alpha$ pathways varied from −2.66 to −0.35 kcal/mol. Therefore, it can be confirmed that the $R_{add}6$ pathway had difficulty occurring due to the highest barrier ($\Delta E = 1.87$ kcal/mol). The reactant complexes (RC) could be found for the R_{add}1-6 pathways, in which the ·OH was perpendicular to the benzene ring. Except for the great change in C−O bond length, all the other RC bonds are close to the reactants, and the RC energies were lower than the reactants by about 2 kcal/mol. However, for R_{abs} pathways, all seven pathways were found to be barrier processes (Fig. 1b and Table S2). Except for the aliphatic-H-abstraction pathway ($R_{abs}\alpha$), the ΔEs of these pathways were all positive, falling between 0.23 and 1.02 kcal/mol. The ΔE of the $R_{abs}\alpha$ pathway was about 1.4−2.0 kcal/mol lower than other abstraction pathways, and ΔE_p was about −12.0 kcal/mol higher than other pathways, indicating that $R_{abs}\alpha$ pathway would be more favorable pathway among H-abstraction pathways from thermodynamical and dynamical aspect.

3.1.2. Reaction kinetics and half-life

To better understand the contribution of styrene transformation products to the atmosphere during the oxidation process, the rate constants (k) and branching ratios (Γ) of total OH-addition and H-abstraction pathways were calculated within the atmospheric temperature range of 216−298 K (Table S2 and Fig. S5). The rate constants of total OH-addition (k_{add}) and H-abstraction (k_{abs}) pathways were 1.81×10^{-10} and 9.43×10^{-12} cm^3 molecule^{-1} s^{-1} at 298 K, respectively. This suggests that H-abstraction pathways were more difficult to happen in the atmosphere than OH-addition pathways, because the difference between k_{add} and k_{abs} was approximately 20 times. The Γ of OH-addition pathway was almost equal to 1 within the temperature range of 216−298 K (Fig. S5). The obtained kinetic results were consistent with the conclusion that OH-addition pathways are the most important pathways. Therefore, OH-addition pathways will be mainly focused on in the following study.

Table S3 shows that the overall rate constant calculated at the B3LYP/6-311+G(3df, 3pd)//B3LYP/6-311G (d, p) level was 19.1×10^{-11} cm^3 molecule^{-1} s^{-1} at 298 K, perfectly matching 10.6×10^{-11} cm^3 molecule^{-1} s^{-1} deduced by Grosjean and Williams (1992) but slightly higher than $(5.87 \pm 0.15) \times 10^{-11}$ cm^3 molecule^{-1} s^{-1} measured by Atkinson and Aschmann (1988). Our results further confirmed that the B3LYP level is reliable for computing the titled reaction, and that the calculated results were credible. Table S3 shows that the rate constant of 3.16×10^{-10} cm^3 molecule^{-1} s^{-1} at 216 K is 1.9 times larger than that at 298 K. This means that the rate constants decrease with increased temperature. The negative temperature dependence could be found in the initial reaction of styrene with ·OH, indicating that increased temperature reduces styrene-OH oxidation reactivity. To provide theoretical reference information for further laboratory investigations, the modified Arrhenius formulas were deduced within the temperature range of 216−298 K (Table S4). That is, the pre-exponential factor, activation energy, and rate constants can be obtained without experimental data at a given temperature using Arrhenius formulas. The total reaction equation is $k_{OH}(T) = (2.05 \times 10^{-29})T^{6.47}\exp(2038/T)$. From the equation, the activation energy of the reaction of styrene with ·OH was estimated to be −4.05 kcal/mol, suggesting that styrene will readily react with ·OH in atmospheric environments.

To in depth understand the yield of major products, the temperature dependence Γs of each OH-addition pathway is drawn in Fig. S6. As shown, the Γ of R_{add}2, 4, 6 pathways were below 4%, indicating that these three pathways contributed much less to the overall rate constant and had difficulty occurring in the atmosphere. For clarity, the Γs of other pathways ($\Gamma_{add}\alpha$, β, 1, 3, and 5) are presented in Fig. 2. The $R_{add}\beta$ pathway dominated the initial reaction within the full temperature range, although the $R_{add}\alpha$ pathway contribution increased at lower temperature. As illustrations, $\Gamma_{add}\alpha$ were 23.8% at 216.69 K and 7.84% at 298.15 K, respectively. The Γs for R_{add}1, R_{add}3 and R_{add}5 were 6.35%, 9.94%, and 6.57% at 298 K, respectively, and these Γs increased subtlety with decreasing temperature. For example, the Γs were 11.8% for R_{add}1, 15.60% for R_{add}3, and 12.50% for R_{add}5 at 216.69 K, respectively. Therefore, the $R_{add}\beta$ pathway was the main pathway, and $IM_{add}\beta$ could be formed as the first major intermediate within the investigated temperature range.

The $\tau_{1/2}$ of styrene reacted with ·OH was also calculated to estimate the atmospheric lifetime of styrene under different atmospheric conditions, because OH-initiated reactions will predominantly control the lifetime of styrene (Guo et al., 2012). The results of $\tau_{1/2}$ are listed in Table S5 and Fig. 3, using the different [·OH] (·OH concentration) at the global average value of 9.70×10^5–1.50×10^7 molecule cm^3 in Guangzhou (Prinn et al., 2001), which is a highly OH-polluted area (Hofzumahaus et al., 2009). As shown in Fig. 3, the $\tau_{1/2}$ decreased from 62.50 to 4.04 min as the [·OH] decreased from 9.70×10^5 to 1.50×10^7 molecule cm^{-3} at ground level. This indicates that styrene could be easily degraded by ·OH at ground level, especially given higher styrene concentrations in industrialized areas of developing countries. For instance, $\tau_{1/2}$ of Guangzhou was only 2.44−4.04 min in the atmosphere, although the $\tau_{1/2}$ increased with increasing altitudes. Therefore, styrene-OH oxidation reactions could be more significant in the atmospheric surface layer; the impact of this reaction on the ambient atmosphere and on human health warrants investigation. To further confirm which one was the major product of the initial reaction, the $\tau_{1/2}$s of $R_{add}\beta$ and $R_{add}\alpha$ were also calculated (Table S6). It can be found that the $\tau_{1/2}$ of $R_{add}\beta$

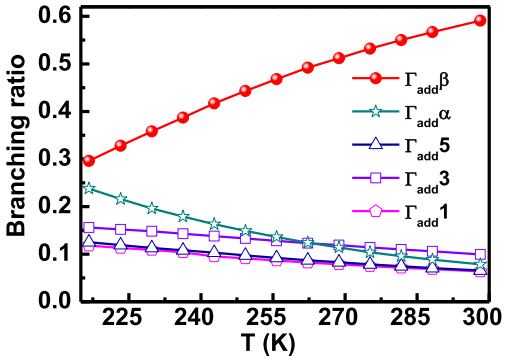

Fig. 2. Branching ratios of each OH-addition pathway.

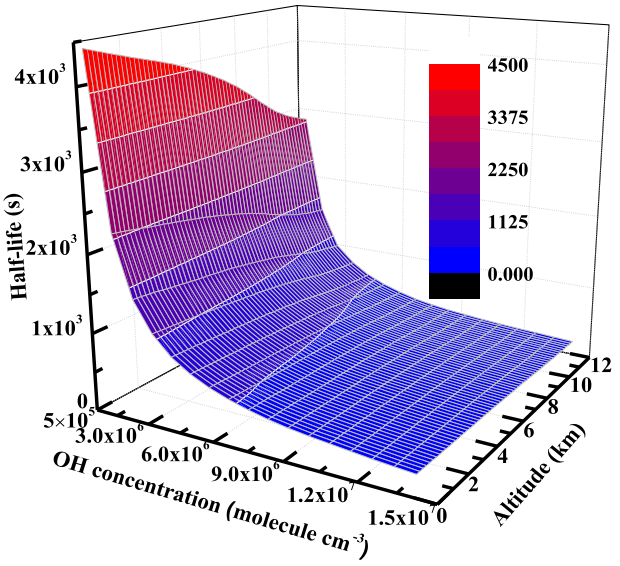

Fig. 3. Plot of the half-life of the styrene reaction with ˙OH as a function of ˙OH concentrations and the altitude range of 0–12 km.

and $R_{add}\alpha$ increased with increased altitudes. At the ground level with [˙OH] = 9.70 × 10^5 molecule cm^{-3}, the $\tau_{1/2}$ of $R_{add}\beta$ was 111.31 min and 7 times larger than that of $R_{add}\alpha$. Even [˙OH] up to 1.5 × 10^7 molecule cm^{-3}, the $\tau_{1/2}$ of $R_{add}\beta$ pathway was still 7 times larger than that of $R_{add}\alpha$. This means that $R_{add}\beta$ pathway is the preferred one in the atmosphere, and the $IM_{add}\beta$ would be an exclusive intermediate for the initial reaction of styrene with ˙OH.

Table 1
Potential barriers ΔE (kcal/mol), reaction heats ΔE_P (kcal/mol) and rate constants k at 298.15 K for subsequent reaction of $IM_{add}\beta$.

Reaction	ΔE[a]	ΔE_p[a]	$k_{298.15\ K}$
$IM_{add}\beta+O_2 \rightarrow$ IMOO	–	−15.08	8.39×10^{-11}[b]
$IM_{add}\beta+O_2 \rightarrow$ IM1B	16.93	14.98	1.39×10^{-28}[b]
$IM_{add}\beta+O_2 \rightarrow$ M1C + HO_2	11.55	−8.91	4.57×10^{-24}[b]
$IM_{add}\beta \rightarrow$ IM1D	38.77	14.88	4.67×10^{-37}[c]

[a] Calculated at B3LYP/6-311+G(3df, 3pd)//B3LYP/6-311G(d,p) level.
[b] The bimolecular rate constants are in units of cm^3 $molecule^{-1}$ s^{-1}.
[c] The unimolecular rate constant is in unit of s^{-1}.

3.2. The formation possibility of SOA in the presence and absence of NO

3.2.1. Formation of peroxy radical

Based on the discussion above, it is clear that $IM_{add}\beta$ was the major intermediate of the initial reactions of styrene with ˙OH in the atmosphere, and could undergo subsequent reactions to produce more stable products. Therefore, the subsequent reactions of $IM_{add}\beta$ with O_2 were investigated to estimate SOA formation possibility. The probable pathways are presented in Fig. 4, including the potential barriers ΔE and reaction heats (ΔE_p). As shown, $IM_{add}\beta$ had difficulty undergoing an isomerization reaction (R_D) to form alcoxyl radical (IM1D), because R_D had to overcome a high ΔE of 38.77 kcal/mol and absorb high ΔE_p of 14.88 kcal/mol. However, $IM_{add}\beta$ could be readily attacked by O_2, undergoing O_2-aliphatic-addition (R_A), O_2-benzene-addition (R_B), and O_2-aliphatic-abstraction (R_C) pathways. The ΔEs for R_B and R_C pathways had a high ΔE of 16.93 and 11.55 kcal/mol; therefore the barrierless pathway R_A would obviously be a dominant pathway, with strong exothermic energy of −15.08 kcal/mol. As such, the IMOO peroxy radical would

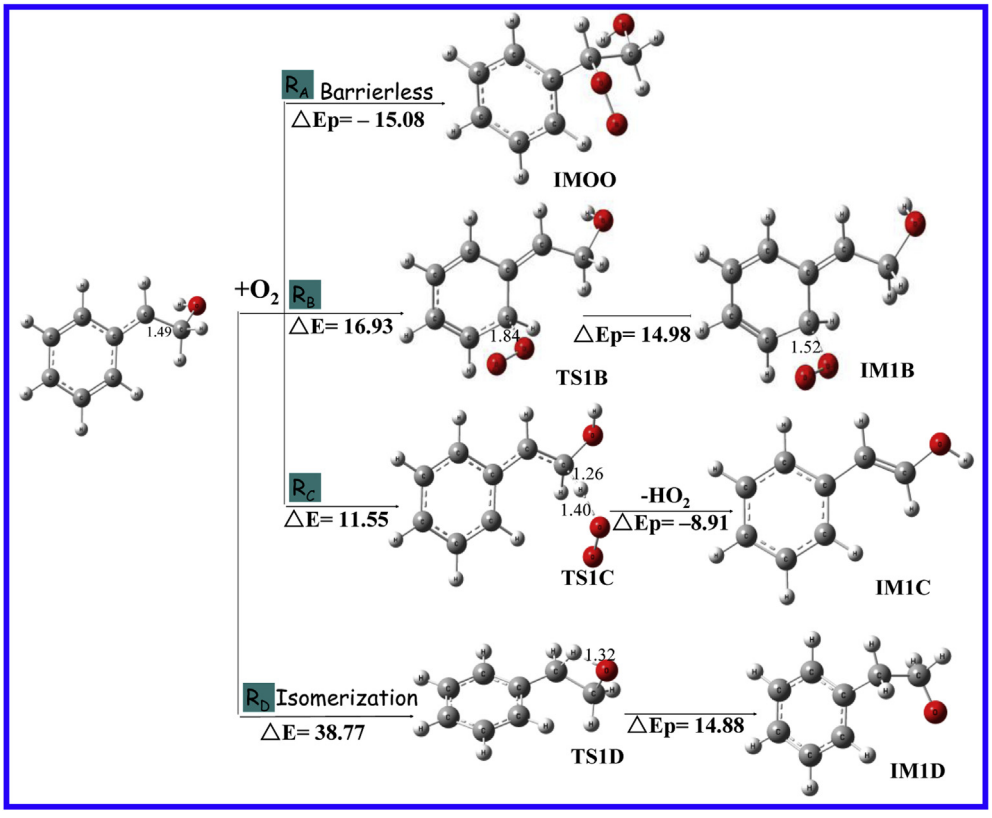

Fig. 4. Possible subsequent reaction pathways for $IM_{add}\beta$.

be produced exclusively by R_A pathway, also observed experimentally (Atkinson and Arey, 2003). The kinetic data further confirm the results mentioned above (Table 1). The R_A, R_B, R_C, and R_D rate constants were calculated to be 8.43×10^{-11}, 1.39×10^{-28}, 4.57×10^{-24} cm^3 molecule^{-1} s^{-1}, and 4.67×10^{-37} s^{-1}, respectively. The R_A rate constant was at least 13 orders of magnitude higher than other three pathways. Therefore, we conclude that the IMOO peroxy radical formation is the most favorable pathway.

The $\tau_{1/2}$s for the IMOO peroxy radical formation were calculated at different altitudes with the corresponding O_2 concentration [O_2] (Gallagher and Hackett, 2004). The results are listed in Table 2, where the altitudes were selected from 0 to 6 km because the styrene-OH oxidation reaction was significant at these lower altitudes. There is an increase in $\tau_{1/2}$ with an altitude increase, but the increase of $\tau_{1/2}$ was slight. For example, the $\tau_{1/2}$ varied from 1.60×10^{-9} to 2.95×10^{-9} s within the altitude range of 0–6 km. This indicated that IMOO would be easily produced once the intermediates $IM_{add}\beta$ encountered O_2 in the atmosphere. Regardless of altitude, the intermediates $IM_{add}\beta$ were more likely to transform into IMOO peroxy radical in the atmosphere. Most of them can be readily attacked by NO to form SOA (Chan et al., 2010) due to highly reactivity of peroxy radicals. This is particularly true in the severely NO-polluted regions, such as the Pearl River Delta region of Southern China, where styrene and NO are abundant in the atmosphere.

3.2.2. Formation possibility of SOA in the absence of NO

As a comparative study, the possible subsequent pathways of IMOO peroxy radicals reacted with NO in absence of NO are shown in Fig. 5 (solid line), to model clear atmosphere without NO pollution. IMOO could undergo an intramolecular hydrogen shift from the hydroxyl group to the peroxy radical site via six-membered ring transition state (TS1B) and then form the weakly bound radical intermediate (IM1B). It can be found that IM1B and TS1B are almost identical in structure due to the energy of IM1B was only 0.52 kcal/mol higher than that of TS1B. The corresponding ΔE and ΔE_P were calculated to be 18.53 and 19.05 kcal/mol, respectively. Nevertheless, the lowest barrier among the intramolecular hydrogen shift was at least 25–35 kcal/mol (Kuwata et al., 2007; Liu et al., 2009), indicating that this pathway can occur easily at ambient environment. Subsequently, IM1B could dissociate immediately to form recycled ˙OH, HCHO, and benzaldehyde, given no barrier ΔE (0.99 kcal/mol) and high exothermic energy (−42.25 kcal/mol). Recycled ˙OH could be generated in the absence of NO, producing secondary pollution. Taraborrelli et al. (Taraborrelli et al., 2012) pointed out that night-time OH-recycling in VOC chemistry can even exceed 100% and is dominated by the reactions following VOC ozonolysis. Therefore, additional OH-recycling would facilitate styrene degradation and peroxy radical decomposition, to form more and more aldehydes. Aldehydes have been widely proven to be an important SOA precursor (Chan et al., 2010; Jang and Kamens, 2001). This means that the IMOO peroxy radical decomposition will be significant and the styrene-OH oxidation reaction will be a potential source of SOA formation in the NO-unpolluted atmosphere.

Table 2
Calculated rate constants and half-life for O_2 addition to $IM_{add}\beta$ pathway at different heights[a] in earth's atmosphere.

h (km)	T (K)	[b]O_2 (molecule cm^{-3})	K (cm^3 molecule^{-1} s^{-1})	Half-life (s)
0	298.15	5.15×10^{18}	8.39×10^{-11}	1.60×10^{-9}
1	281.7	4.84×10^{18}	8.15×10^{-11}	1.76×10^{-9}
2	275.21	4.38×10^{18}	8.06×10^{-11}	1.96×10^{-9}
3	268.72	3.95×10^{18}	7.96×10^{-11}	2.20×10^{-9}
4	262.23	3.56×10^{18}	7.87×10^{-11}	2.47×10^{-9}
5	255.74	3.20×10^{18}	7.77×10^{-11}	2.79×10^{-9}
6	249.25	3.06×10^{18}	7.67×10^{-11}	2.95×10^{-9}

[a] Temperature drops about 6.49 K for every 1 km increase in altitude. Into the stratosphere (from 11 km height above the earth surface), the constant temperature is 216.69 K (Van den Broeck, 2010).

[b] In the troposphere, the altitude dependence barometric pressure and ambient partial pressure oxygen are derived from the reference (Gallagher and Hackett, 2004).

3.2.3. Formation possibility of SOA in the presence of NO

Fig. 5 (dashed line) also illustrates the subsequent pathways of the IMOO peroxy radical in a simulated NO-polluted atmosphere. It can be found that IMOO could be immediately removed by NO, forming energy-rich intermediate (IM–OH–ONO_2), because this pathway was a barrierless processes and the corresponding exothermic energy was −16.96 kcal/mol (Fig. 5). Then, IM–OH–ONO_2 would undergo unimolecular decomposition (R_{dec}) or the isomerization (R_{iso}) pathways. Due to its higher barrier and lower exothermic energy, the R_{dec} pathway was more difficult to occur to form alkoxy radical in the atmosphere. For example, the ΔEs were 24.11 and 28.38 kcal/mol, and the ΔE_Ps were −28.38 and −1.50 kcal/mol for the R_{iso} and R_{dec} pathway, respectively. Furthermore, the R_{dec} rate constant was 1.95×10^{-6} s^{-1} at ground level and 40 times smaller than that of R_{iso} pathways, further confirming that IMOO isomerization could occur exclusively to form $IMONO_2$ and alkoxy radical cannot be produced. Although the ΔE of R_{iso} were up to 24.11 kcal/mol, they were still lower than the energy released from $IM_{add}\beta$ to IMOO and then to IM–OH–ONO_2 (−32.04 kcal/mol). This suggests that R_{iso} pathways could happen spontaneously.

As a result, IMOO + NO dominates to produce organic nitrates (IMO-NO_2) as a main product under high NO_x conditions. Organic nitrates (RO–NO_2) are ubiquitous in the atmosphere, which are also observed in VOCs-NO_x oxidation systems produce SOA with significant yield in chamber studies (Rollins et al., 2010). Therefore, RO–NO_2 plays an important role in SOA production, indicating that styrene-OH oxidation reactions could significantly contribute to SOA formation in the NO-polluted atmosphere. Further chamber measurement and experiment work is highly-needed to confirm these theoretical results.

3.3. Atmospheric gas-particle partitioning of organic nitrate (RO–NO_2)

Generally, the SOA is formed from low-volatility oxidation products, like glyoxal (Lim et al., 2013), isoprene (Lim et al., 2005), acetic acid and methylglyoxal (Tan et al., 2012b) However, multifunctional organic nitrates are known to be major products of the OH initiated atmospheric reaction of styrene in presence of NO, which has sufficiently higher volatility that they are not readily nucleate to form new particles (Perraud et al., 2010). Whereas, the model simulation and the laboratory studies indicated that a large fraction of organo-nitrate groups was formed in aerosol particles (Liu et al., 2012). Therefore, the formation process of product organic nitrate ultimately leading to the formation of the SOA need to be further discussed.

According to the Junge-Pankow and K_{oa} adsorption model, the potential distribution (ϕ) of organic nitrate in the particulate phase can be calculated, and the K_{oa} adsorption model predicts the values of ϕ by.

$$\phi = (K_p C_{TSP})/(1 + K_p C_{TSP}) \quad (1)$$

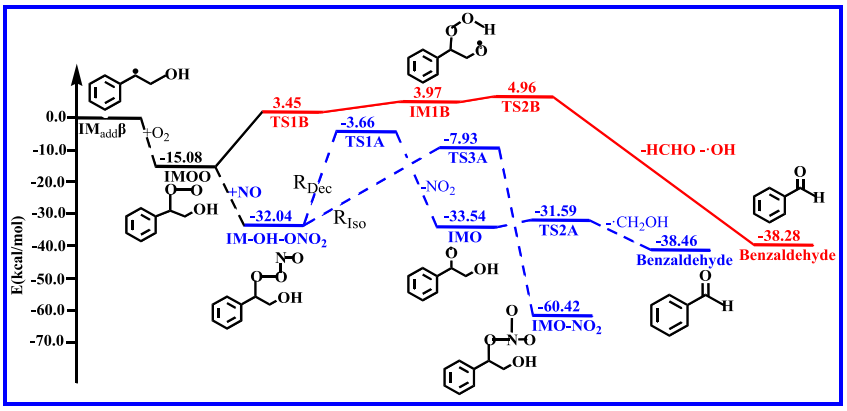

Fig. 5. Profile of potential energy surface for subsequent reaction of the main intermediate $IM_{add}\beta$ under low and high NO conditions. The energy data are given in kcal/mol. (Red solid line represents the absence of NO and blue dashed line represents the presence of NO). (For interpretation of the references to color in this figure legend, the reader is referred to the web version of this article.)

where C_{TSP} is the concentration of total suspended particulates (TSP) in the air (μg m^{-3}), and K_p is the particle/gas partition coefficient. The K_p could be calculated using the equation:

$$\log K_p = \log K_{oa} + \log f_{OM} - 11.91 \quad (2)$$

where $\log K_{oa}$ is the octanol–air partitioning coefficient, and $\log f_{OM}$ is the fraction of organic matter. The organic carbon contents of particles in this study were assumed as ~0.58 of organic matter (Ranney, 1969). According to the model, the relationship of particulate fraction and $\log K_{oa}$ can be obtained. For the different scenarios have been used in this model, the values range of f_{OM} (from 0.2 to 0.4) and C_{TSP} (from 100 to 300 μg/m^3) can be found in the atmosphere of Guangzhou city (Ma et al., 2010). The values of $\log K_{oa}$(8.918) and K_p(2.03×10^{-4}) of organic nitrate could be estimated using the Estimation Program Interface (EPI) suite (EPI-suite, 2012). And the TSP concentration in the Guangzhou was quoted from the reference (Ma et al., 2010). According to Eq. (1), the percent of organic nitrate in the particulate phase was calculated in the range of 2.4%–6.3% in Guangzhou city (Fig. 6 and Table S7). It can be easily seen that the K_{oa} adsorption model slightly overestimated the sorption of organic nitrate, and the derivation between the modeling and the calculated data in this study was possible due to different parameter values for different aerosol types. Besides, the uptake coefficient of organic nitrate adsorbed on to the airborne particle also could reach to 1.6% (EPI-suite, 2012).

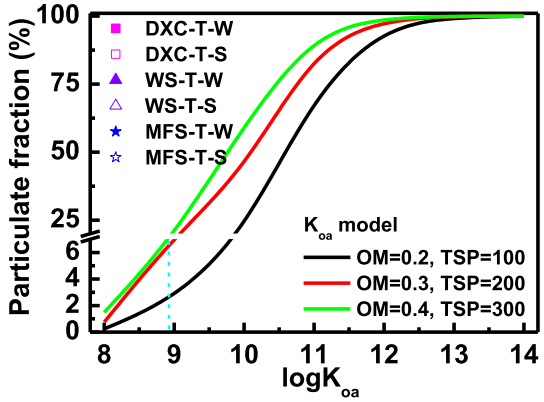

Fig. 6. Comparison of the calculated particulate fractions of organic nitrate with predictions of the K_{oa} adsorption model. (DXC-T-W/S, WS-T-W/S and MFS-T-W/S represent the winter/summer in Daxuecheng, Wushan, and Maofengshan sampling sites of Guangzhou city, respectively (Ma et al., 2010)).

3.4. Significance of styrene SOA formation

Organic nitrate yields was estimated up to 30% for the reaction of C_7 peroxy radicals with NO (Atkinson et al., 1987), and the nitrate yields should be increased for larger peroxy radicals (Zhang et al., 2004). According to our above-mentioned calculation results about the rate constants and branching ratios for the formation of organic nitrates, the yield of the product trans-(R(S))-2-hydroxy-1-phenylethyl nitrate (RO-NO_2) was estimated as 54.9%, with vapor pressure 1.51×10^{-2} Pa at 298 K. As for the dominated products in this system, organic nitrate, formaldehyde, benzaldehyde as well as the oligomers, most of them are not SOA-formation product. Therefore, the total SOA yield of this system can not be completely estimated. However, an observation on the ambient aerosol in Los Angeles identified aerosol organic nitrate and indicated that organic nitrates might constitute an important fraction of the total organic aerosol load (Presto et al., 2005). Therefore, we can speculate that the mass concentration of air organic nitrates dominate the total organic nitrates in this OH-initiated oxidation system (Perraud et al., 2012).

3.5. Environmental implications

Our research shows that organic nitrate plays a very important role in SOA formation. And the percent of organic nitrate in the particulate phase was calculated within the range of 2.4%–6.3% in Guangzhou city. To better understand the effect of NO on organic nitrate formation, the $\tau_{1/2}$ for the reaction of IMOO and NO at altitudes ranging from 0 to 6 km was also measured (Table S8) within the NO concentration range from 1 ppbv (2.69×10^{10} molecule cm^{-3}) to 35 ppbv (9.42×10^{11} molecule cm^{-3}) (Liu et al., 2009). The $\tau_{1/2}$ increased with increased altitude at a fixed [NO], but the increase was slight.

At [NO] = 2.69×10^{10} molecule cm^{-3}, the $\tau_{1/2}$ increased from 0.32 to 0.35 s within the altitude range of 0–6 km. At ground level with [NO] = 2.69×10^{10} molecule cm^{-3}, the $\tau_{1/2}$ was 0.32 s and decreased to 9.14×10^{-3} s at [NO] = 9.42×10^{11} molecule cm^{-3}. This indicates that IMOO would be easily attacked by NO in a NO-polluted area. In addition, given the relatively short atmospheric residence time of NO, NO sources quite close to IMOO could then produce organic nitrate (RO–NO_2). The short $\tau_{1/2}$ of 10^{-3}–10^{-1} s indicates that the contribution of styrene-OH oxidation reaction to

SOA formation is important, and as such, the identification and quantification of styrene-OH oxidation reaction in atmospheric environment are significant topic deserving of future study, particularly in high NO-polluted area. We are hopeful that this study supports future assessments of the environmental impact of the emission VOCs in diverse atmospheric conditions.

Acknowledgments

This is contribution No. IS–1961 from GIGCAS. This work was financially supported by The Team Project from NSF of Guangdong Province, China (S2012030006604), NSFC (41205088, 41373102 and 21307132), Science and Technology Project of Guangdong Province (2012A032300017) and Shenzhen City (CXZZ20130513160913488). The authors also thank Professor Donald G. Truhlar for providing the POLYRATE program.

Appendix A. Supplementary data

Supplementary data related to this article can be found at http://dx.doi.org/10.1016/j.atmosenv.2014.10.042.

References

An, T.C., Gao, Y.P., Li, G.Y., Kamat, P.V., Peller, J., Joyce, M.V., 2014. Kinetics and mechanism of (OH)-O-center dot mediated degradation of dimethyl phthalate in aqueous solution: experimental and theoretical studies. Environ. Sci. Technol. 48, 641–648.

Atkinson, R., Arey, J., 2003. Atmospheric degradation of volatile organic compounds. Chem. Rev. 103, 4605–4638.

Atkinson, R., Aschmann, S.M., 1988. Kinetics of the reactions of acenaphthene and acenaphthylene and structurally-related aromatic-compounds with OH and NO_3 Radicals, N_2O_5 and O_3 at 296+/-2 K. Int. J. Chem. Kinet. 20, 513–539.

Atkinson, R., Aschmann, S.M., Winer, A.M., 1987. Alkyl nitrate formation from the reaction of a series of branched RO_2 radicals with NO as a function of temperature and pressure. J. Atmos. Chem. 5, 91–102.

ATSDR, 2007. Agency for Toxic Substances and Disease Registry: Toxicological Profile for Styrene. Department of Health and Human Services, Public Health Service, Atlanta, GA.

Baxter, C.S., Warshawsky, D., 2012. Styrene, polyphenyls, and related compounds. In: Bingham, E., Cohrssen, B. (Eds.), Patty's Toxicology, sixth ed. John Wiley & Sons, Inc, pp. 221–242.

Bignozzi, C.A., Maldotti, A., Chiorboli, C., Bartocci, C., Carassiti, V., 1981. Kinetics and mechanism of reactions between aromatic olefins and hydroxyl radicals. Int. J. Chem. Kinet. 13, 1235–1242.

Chan, A.W.H., Chan, M.N., Surratt, J.D., Chhabra, P.S., Loza, C.L., Crounse, J.D., Yee, L.D., Flagan, R.C., Wennberg, P.O., Seinfeld, J.H., 2010. Role of aldehyde chemistry and NO_x concentrations in secondary organic aerosol formation. Atmos. Chem. Phys. 10, 7169–7188.

Clapp, L.J., Jenkin, M.E., 2001. Analysis of the relationship between ambient levels of O_3, NO_2 and NO as a function of NO chi in the UK. Atmos. Environ. 35, 6391–6405.

Corchado, J.C., Chang, Y.-Y., Fast, P.L., Villa, J., Hu, W.-P., Liu, Y.-P., Lynch, G.C., Nguyen, K.A., Jackels, C.F., Melissas, V.S., Lynch, B.J., Rossi, I., Coitino, E.L., Fernandez-Ramos, A., Pu, J.-Z., Albu, T.V., Steckler, R., Garrett, B.C., Isaacson, A.D., Truhlar, D.G., 2002. POLYRATE Version 9.1. University of Minnesota, Minneapolis.

EPA, 2013. The Original List of Hazardous Air Pollutants. http://www.epa.gov/ttn/atw/orig189.html.

EPI-suite, 2012. Estimation Programs Interface Suite™ for Microsoft® Windows, v. 4.11. United States Environmental Protection Agency, Washington, DC, USA.

Fernandez-Ramos, A., Ellingson, B.A., Garret, B.C., Truhlar, D.G., 2007. Variational transition state theory with multidimensional tunneling. Rev. Comput. Chem. 23, 125–232. Wiley-VCH: Hoboken, NJ, 2007.

Frisch, M.J., Truck, G.W., Schlegel, H.B., Scuseria, G.E., Robb, M.A., Cheeseman, J.R., Zakrzewski, V.G., Montgomery, J.A., Stratmann, J.R.E., Burant, J.C., Dapprich, S., Millam, J.M., Daniels, A.D., Kudin, K.N., Strain, M.C., Farkas, O., Tomasi, J., Barone, V., Cossi, M., Cammi, R., Mennucci, B., Pomelli, C., Adamo, C., Clifford, S., Ochterski, J., Petersson, G.A., Ayala, P.Y., Cui, Q., Morokuma, K., Malick, D.K., Rabuck, A.D., Raghavachari, K., Foresman, J.B., Cioslowski, J., Ortiz, J.V., Boboul, A.G., Stefnov, B.B., Liu, G., Liaschenko, A., Piskorz, P., Komaromi, L., Gomperts, R., Martin, R.L., Fox, D.J., Keith, T., AleLaham, M.A., Peng, C.Y., Nanayakkara, A., Gonzalez, C., Challacombe, M., Gill, P.M.W., Johnson, B., Chen, W., Wong, M.W., Andres, J.L., Gonzalez, C., HeadeGordon, M., Replogle, E.S., Pople, J.A., 2003. GAUSSIAN 03, Revision A.1. Guassian, Inc., Pittsburgh, PA.

Fukui, K., 1981. The path of chemical-reactions - the IRC approach. Acc. Chem. Res. 14, 363–368.

Gallagher, S.A., Hackett, P.H., 2004. High-altitude illness. Emerg. Med. Clin. N. Am. 22, 329–355.

Gao, Y.P., Ji, Y.M., Li, G.Y., An, T.C., 2014. Mechanism, kinetics and toxicity assessment of OH-initiated transformation of triclosan in aquatic environments. Water Res. 49, 360–370.

Gonzalezlafont, A., Truong, T.N., Truhlar, D.G., 1991. Direct dynamics calculations with neglect of diatomic differential-overlap molecular-orbital theory with specific reaction parameters. J. Phys. Chem. 95, 4618–4627.

Grosjean, D., Williams, E.L., 1992. Environmental persistence of organic-compounds estimated from structure reactivity and linear free-energy relationships unsaturated aliphatics. Atmos. Environ. A Gen. Top. 26, 1395–1405.

Guo, J., Jiang, Y., Hu, X., Xu, Z., 2012. Volatile organic compounds and metal Leaching from composite products made from fiberglass-resin portion of printed circuit board waste. Environ. Sci. Technol. 46, 1028–1034.

Hofzumahaus, A., Rohrer, F., Lu, K.D., Bohn, B., Brauers, T., Chang, C.C., Fuchs, H., Holland, F., Kita, K., Kondo, Y., Li, X., Lou, S.R., Shao, M., Zeng, L.M., Wahner, A., Zhang, Y.H., 2009. Amplified trace gas removal in the troposphere. Science 324, 1702–1704.

Jang, M.S., Kamens, R.M., 2001. Atmospheric secondary aerosol formation by heterogeneous reactions of aldehydes in the presence of a sulfuric acid aerosol catalyst. Environ. Sci. Technol. 35, 4758–4766.

Ji, Y.M., Gao, Y.P., Li, G.Y., An, T.C., 2012. Theoretical study of the reaction mechanism and kinetics of low-molecular-weight atmospheric aldehydes (C1–C4) with NO_2. Atmos. Environ. 54, 288–295.

Ji, Y.M., Wang, H.H., Gao, Y.P., Li, G.Y., An, T.C., 2013. A theoretical model on the formation mechanism and kinetics of highly toxic air pollutants from halogenated formaldehydes reacted with halogen atoms. Atmos. Chem. Phys. 13, 11277–11286.

Kroll, J.H., Ng, N.L., Murphy, S.M., Flagan, R.C., Seinfeld, J.H., 2005. Secondary organic aerosol formation from isoprene photooxidation under high-NO_x conditions. Geophys. Res. Lett. 32.

Kroll, J.H., Ng, N.L., Murphy, S.M., Flagan, R.C., Seinfeld, J.H., 2006. Secondary organic aerosol formation from isoprene photooxidation. Environ. Sci. Technol. 40, 1869–1877.

Kuwata, K.T., Dibble, T.S., Sliz, E., Petersen, E.B., 2007. Computational studies of intramolecular hydrogen atom transfers in the beta-hydroxyethylperoxy and beta-hydroxyethoxy radicals. J. Phys. Chem. A 111, 5032–5042.

Lim, H.J., Carlton, A.G., Turpin, B.J., 2005. Isoprene forms secondary organic aerosol through cloud processing: model simulations. Environ. Sci. Technol. 39, 4441–4446.

Lim, Y.B., Tan, Y., Turpin, B.J., 2013. Chemical insights, explicit chemistry, and yields of secondary organic aerosol from OH radical oxidation of methylglyoxal and glyoxal in the aqueous phase. Atmos. Chem. Phys. 13, 8651–8667.

Liu, Q., Li, M., Chen, R., Li, Z.Y., Qian, G.R., An, T.C., Fu, J.M., Sheng, G.Y., 2009. Biofiltration treatment of odors from municipal solid waste treatment plants. Waste Manag. 29, 2051–2058.

Liu, S., Shilling, J.E., Song, C., Hiranuma, N., Zaveri, R.A., Russell, L.M., 2012. Hydrolysis of organonitrate functional groups in aerosol particles. Aerosol Sci. Technol. 46, 1359–1369.

Ma, S.X., Peng, P.A., Song, J.Z., Zhao, J.P., He, L.L., Sheng, G.Y., Fu, J.M., 2010. Stable carbon isotopic compositions of organic acids in total suspended particles and dusts from Guangzhou, China. Atmos. Res. 98, 176–182.

Molina, V., Smith, B.R., Merchan, M., 1999. A theoretical study of the electronic spectrum of styrene. Chem. Phys. Lett. 309, 486–494.

Na, K., Song, C., Cocker, D.R., 2006. Formation of secondary organic aerosol from the reaction of styrene with ozone in the presence and absence of ammonia and water. Atmos. Environ. 40, 1889–1900.

Perraud, V., Bruns, E.A., Ezell, M.J., Johnson, S.N., Greaves, J., Finlayson-Pitts, B.J., 2010. Identification of organic nitrates in the NO_3 radical initiated oxidation of alpha-pinene by atmospheric pressure chemical ionization mass spectrometry. Environ. Sci. Technol. 44, 5887–5893.

Perraud, V., Bruns, E.A., Ezell, M.J., Johnson, S.N., Yu, Y., Alexander, M.L., Zelenyuk, A., Imre, D., Chang, W.L., Dabdub, D., Pankow, J.F., Finlayson-Pitts, B.J., 2012. Nonequilibrium atmospheric secondary organic aerosol formation and growth. Proc. Natl. Acad. Sci. U. S. A. 109, 2836–2841.

Presto, A.A., Hartz, K.E.H., Donahue, N.M., 2005. Secondary organic aerosol production from terpene ozonolysis. 2. Effect of NO_x concentration. Environ. Sci. Technol. 39, 7046–7054.

Prinn, R.G., Huang, J., Weiss, R.F., Cunnold, D.M., Fraser, P.J., Simmonds, P.G., McCulloch, A., Harth, C., Salameh, P., O'Doherty, S., Wang, R.H.J., Porter, L., Miller, B.R., 2001. Evidence for substantial variations of atmospheric hydroxyl radicals in the past two decades. Science 292, 1882–1888.

Ranney, R.W., 1969. An organic carbon-organic matter conversion equation for pennsylvania surface soils. Soil Sci. Soc. Am. Proc. 33, 809–811.

Renbaum, L.H., Smith, G.D., 2009. Organic nitrate formation in the radical-initiated oxidation of model aerosol particles in the presence of NO_x. Phys. Chem. Chem. Phys. 11, 8040–8047.

Rollins, A.W., Fry, J.L., Hunter, J.F., Kroll, J.H., Worsnop, D.R., Singaram, S.W., Cohen, R.C., 2010. Elemental analysis of aerosol organic nitrates with electron ionization high-resolution mass spectrometry. Atmos. Meas. Tech. 3, 301–310.

Seta, T., Nakajima, M., Miyoshi, A., 2006. High-temperature reactions of OH radicals with benzene and toluene. J. Phys. Chem. A 110, 5081–5090.

Sloane, T.M., Brudzynski, R.J., 1979. Competition between reactive sites in the reactions of oxygen atoms and hydroxyl radicals with phenylacetylene and styrene. J. Am. Chem. Soc. 101, 1495–1499.

Sun, X.Y., Hu, Y.M., Xu, F., Zhang, Q.Z., Wang, W.X., 2012. Mechanism and kinetic studies for OH radical-initiated atmospheric oxidation of methyl propionate. Atmos. Environ. 63, 14–21.
Tan, J.H., Guo, S.J., Ma, Y.L., Yang, F.M., He, K.B., Yu, Y.C., Wang, J.W., Shi, Z.B., Chen, G.C., 2012a. Non-methane hydrocarbons and their ozone formation potentials in foshan, China. Aerosol Air Qual. Res. 12, 387–398.
Tan, Y., Lim, Y.B., Altieri, K.E., Seitzinger, S.P., Turpin, B.J., 2012b. Mechanisms leading to oligomers and SOA through aqueous photooxidation: insights from OH radical oxidation of acetic acid and methylglyoxal. Atmos. Chem. Phys. 12, 801–813.
Taraborrelli, D., Lawrence, M.G., Crowley, J.N., Dillon, T.J., Gromov, S., Gross, C.B.M., Vereecken, L., Lelieveld, J., 2012. Hydroxyl radical buffered by isoprene oxidation over tropical forests. Nat. Geosci. 5, 190–193.
Tuazon, E.C., Arey, J., Atkinson, R., Aschmann, S.M., 1993. Gas-phase reactions of 2-Vinylpyridine and styrene with OH and NO_3 radicals and O_3. Environ. Sci. Technol. 27, 1832–1841.
Uhde, E., Salthammer, T., 2007. Impact of reaction products from building materials and furnishings on indoor air quality – a review of recent advances in indoor chemistry. Atmos. Environ. 41, 3111–3128.
Van den Broeck, C., 2010. Thermodynamics of information: bits for less or more for bits? Nat. Phys. 6, 937–938.
Zhang, J.Y., Dransfield, T., Donahue, N.M., 2004. On the mechanism for nitrate formation via the peroxy radical plus NO reaction. J. Phys. Chem. A 108, 9082–9095.